Reionization epoch and cosmic dawn with the 21-cm redshifted line

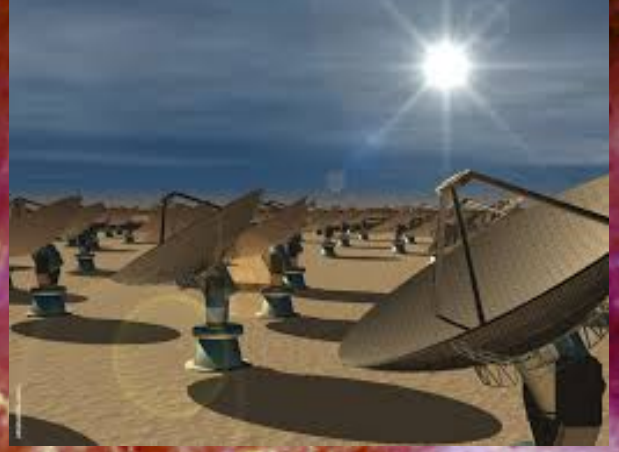

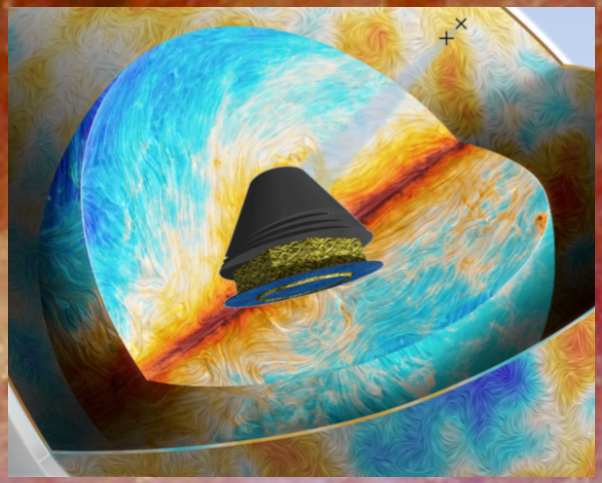

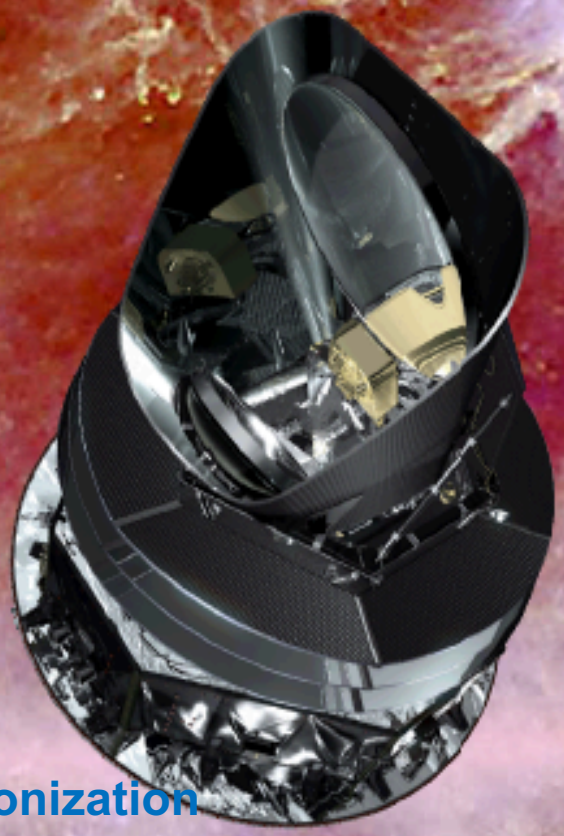

Carlo Burigana
in collaboration with Tiziana Trombetti
INAF-IRA Bologna

Mainly based on "Perspectives for cosmological reionization from future CMB and radio projects", by TT & CB, will appear on Frontiers

June 26-27, 2018 – Ferrara, COSMOS Meeting on Astropart. & Fund. Phys. with CMB

Abstract / Outline - I

- **Planck satellite results: cosmological reionization scenarios almost compatible with astrophysical models for the evolution of structure, galaxy and star formation**

- **The full understanding of the dawn age and of the reionization and thermal history since recombination epoch is still far to be consolidated**

- **Relevance for the comprehension of early phases of structure formation and evolution and connection with a large variety of astrophysical and cosmological questions →**

- **Important to discriminate among the various models compatible with current data**

✓ **21-cm line tomographic view allows to reconstruct ionization and clumping history**

Abstract / Outline - II

- **Few comments about CMB information on reionization:**
  - ✓ **Polarization anisotropies**
  - ✓ **Spectrum**

- **Brief overview of:**
  - **Radio (namely the SKA and its precursor/pathfinders) projects**

- **Their scientific outcomes, focussing on the information carried out by:**
  - ➢ **redshifted 21-cm line radio emission**

- **Contribution of future radio surveys to foreground mitigation for reionization studies with CMB polarization**
  - ✓ **Galactic foregrounds**
  - ✓ **Extragalactic foregrounds**

E and B modes from cosmological reionization models

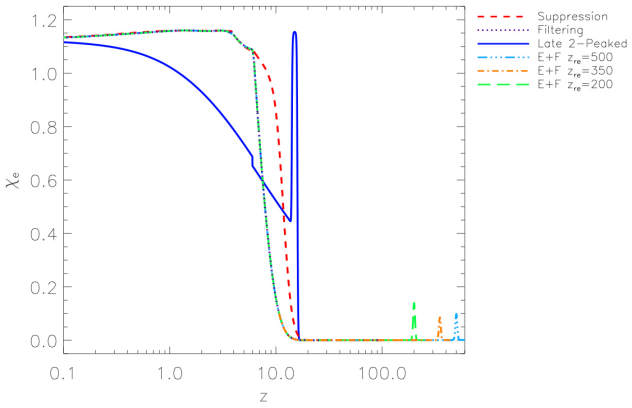

Different ionization histories produce different CMB APS, affecting mainly

- ✓ E, B polarization modes
- ✓ TE cross-correlation mode

Boltzmann codes (e.g. CAMB) predict APS
Modified versions for modelling histories

- ➢ **Reionization bump at low l (about z_reion$^{1/2}$) for "late" processes**
- ➢ **Intermediate/high l effects for early reionization**

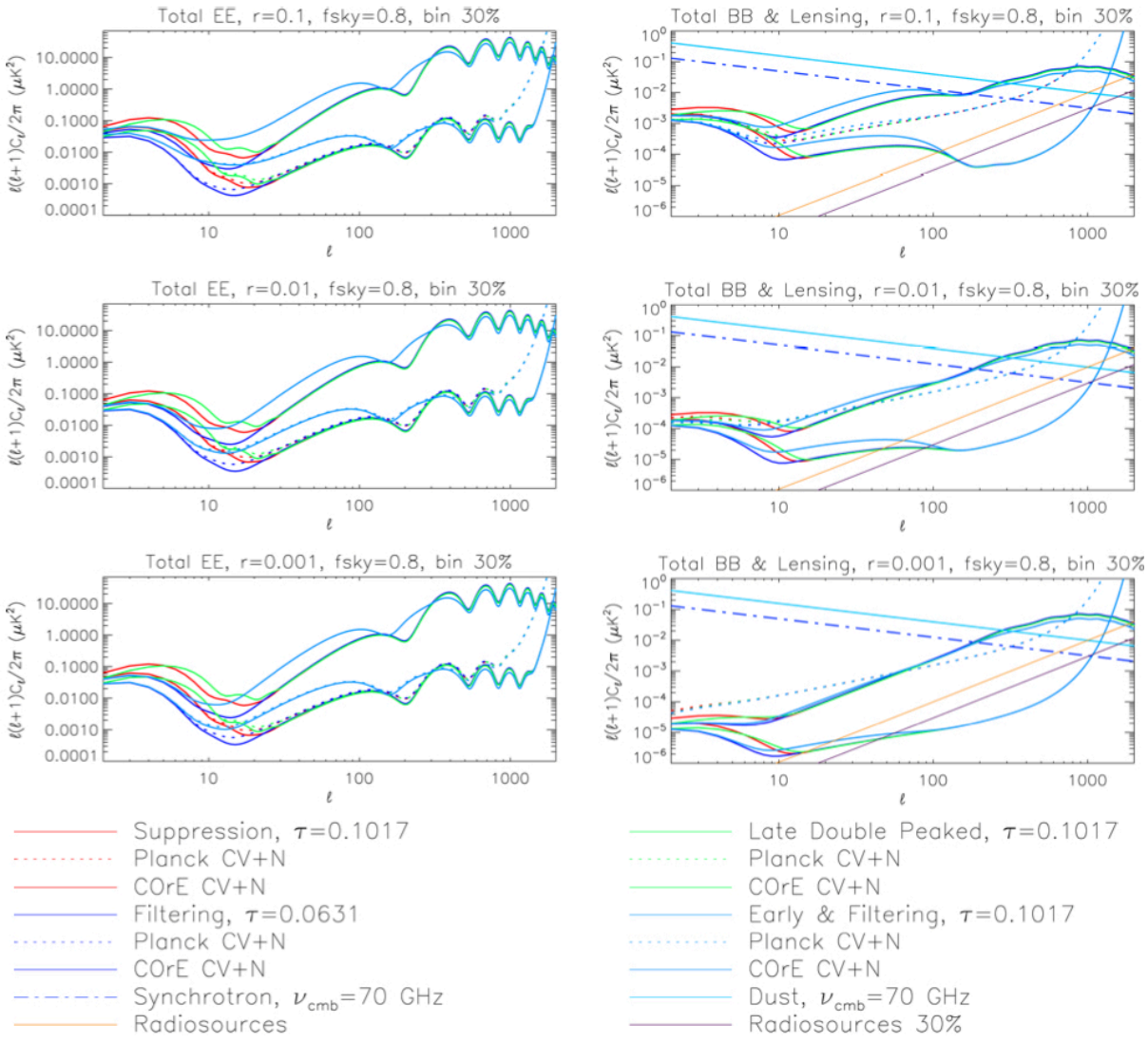

Trombetti & Burigana 2012, JMP

First luminous sources in the Universe & cosmological reionization from Planck

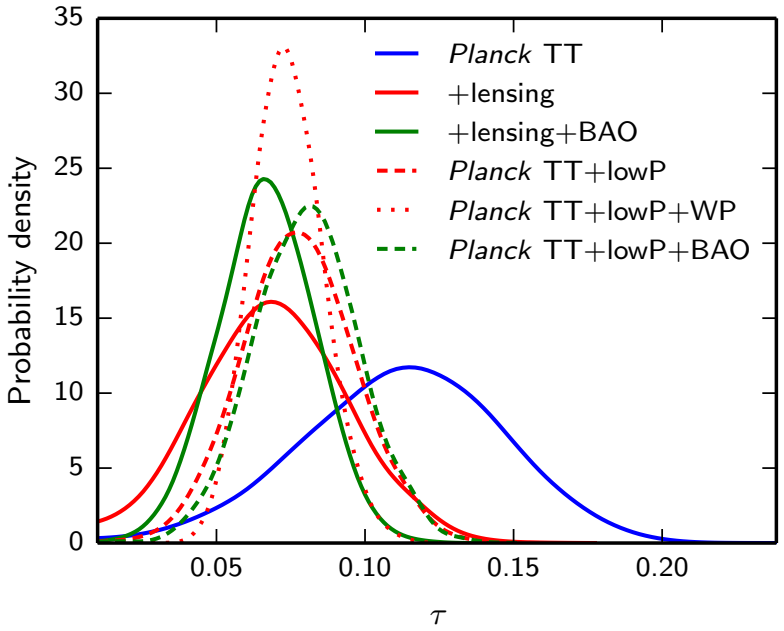

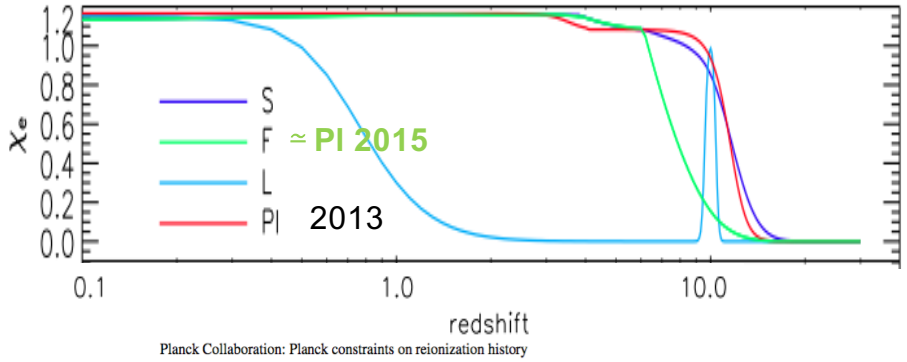

Planck Collaboration: Planck constraints on reionization history

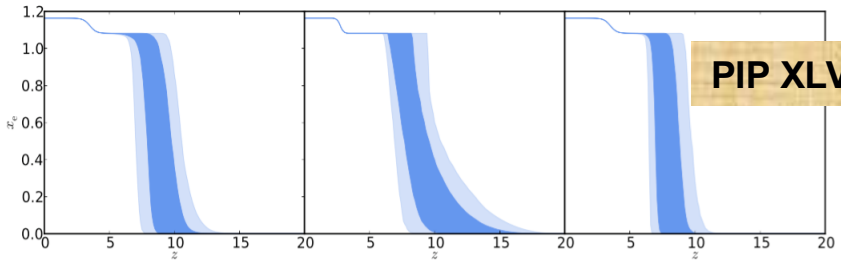

PIP XLVII, 2016

Fig. 18. Constraints on ionization fraction during reionization. The allowed models, in terms of z_{re} and Δz, translate into an allowed region in $x_e(z)$ (68 % and 95 % in dark blue and light blue, respectively), including the $z_{end} > 6$ prior here. *Left*: Constraints from CMB data using a redshift-symmetric function ($x_e(z)$ as a hyperbolic tangent with $\delta z = 0.5$). *Centre*: Constraints from CMB data using a redshift-asymmetric parameterization ($x_e(z)$ as a power law). *Right*: Constraints from CMB data using a redshift-symmetric parameterization with additional constraints from the kSZ effect.

WP (WMAP 9) reanalysed with *Planck* dust emission maps

$$\tau = 0.066 \pm 0.0016 \quad z_{\rm re} = 8.8^{+1.7}_{-1.4} \quad (68\,\%{\rm CL}\,, \textit{Planck}\,{\rm TT} + {\rm lensing} + {\rm lowP})$$

$$\tau = 0.074^{+0.011}_{-0.013} \quad z_{\rm re} = 9.6 \pm 1.1 \quad (68\,\%{\rm CL}\,, \textit{Planck}\,{\rm TT} + {\rm lowP} + {\rm WP})$$

More accurate CMB polarization measurements → reionization history reconstruction

"beyond the τ approximation"

- ✓ "blind" methods" (e.g. principal component method, reconstruction of χ_e in z bins)
- ✓ estimation (e.g. with MCMC methods) of physical / phenomenological reionization model parameters

CMB spectrum: current status

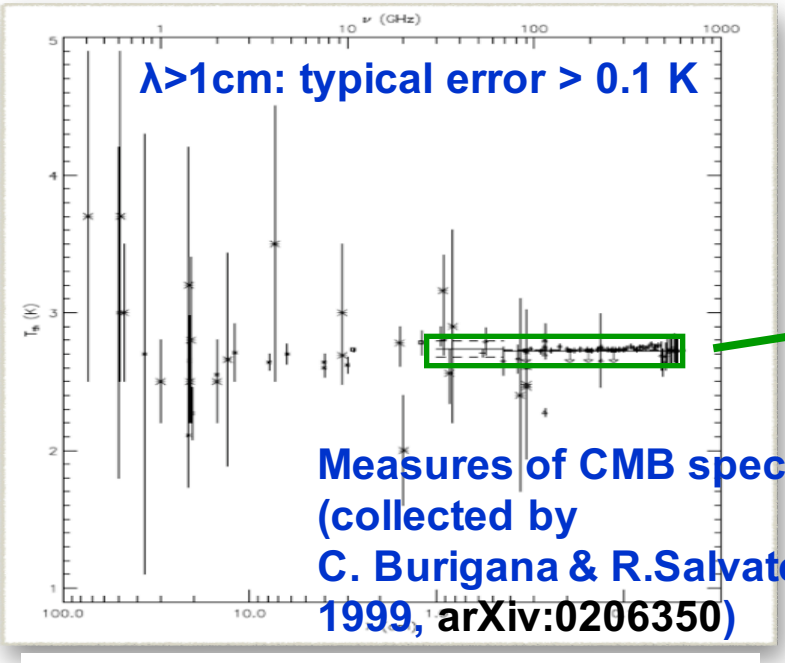

$T_0 = 2.725$
± 0.002 °K

Mather, J.C.,
et al., 1999,
ApJ, 512, 511

FIRAS
measures:
typical error
±0.0001 K

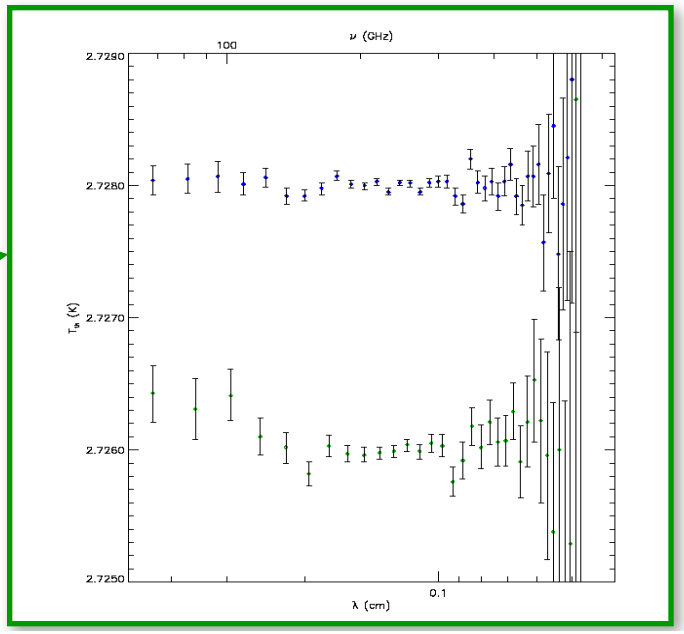

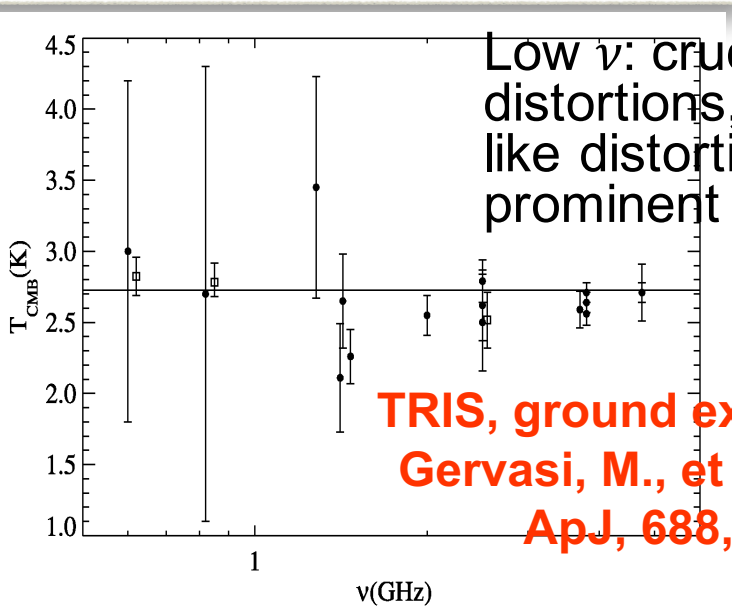

Low ν: crucial for free-free distortions, where Bose-Einstein like distortions are also more prominent

TRIS, ground experiment
Gervasi, M., et al. 2008,
ApJ, 688, 24

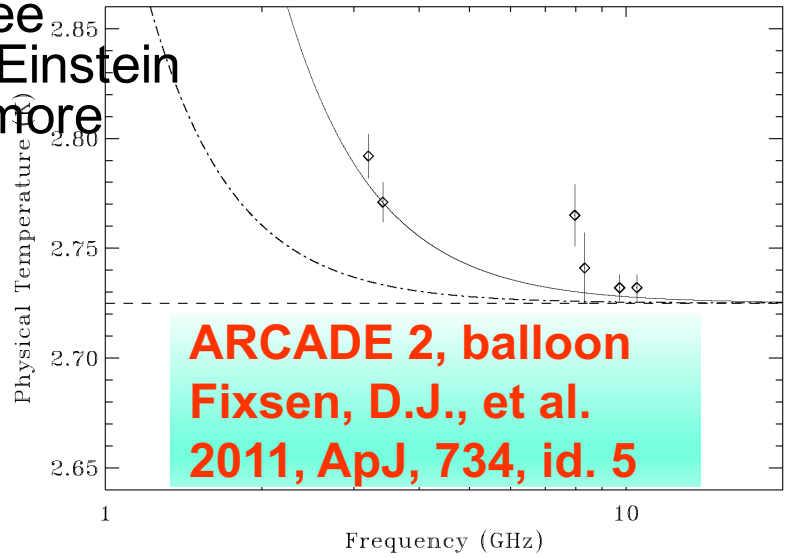

ARCADE 2, balloon
Fixsen, D.J., et al.
2011, ApJ, 734, id. 5

FIG. 5.—CMB thermodynamic temperature measured at low frequencies (see

SKA
&
precursors/pathfinders

SKA & precursors/pathfinders

The **SKA will be a giant radio telescope** with

- effective collecting area of **one-million square meters** observing in the radio band with different antenna concepts
- continuous frequency coverage from **50 MHz to 14 GHz**

Low *ν*: Western Australia

Mid & High *ν*: Southern Africa

allowing (Maartens et al., 2015)

- **very wide sky surveys**
- **redshift depth observations or possibly at higher frequencies up to 25 GHz a range typically accessible from the ground (Barbosa et al., 2012)**

- In 2008, the SKA Science and Engineering Committee, SSEC, recognized in the

✓ **"Precursors"** designation the telescopes built on one of the two SKA candidate sites, Australia or South Africa

✓ **"Pathfinders"** classification all SKA-related technology, science and operations activity telescopes

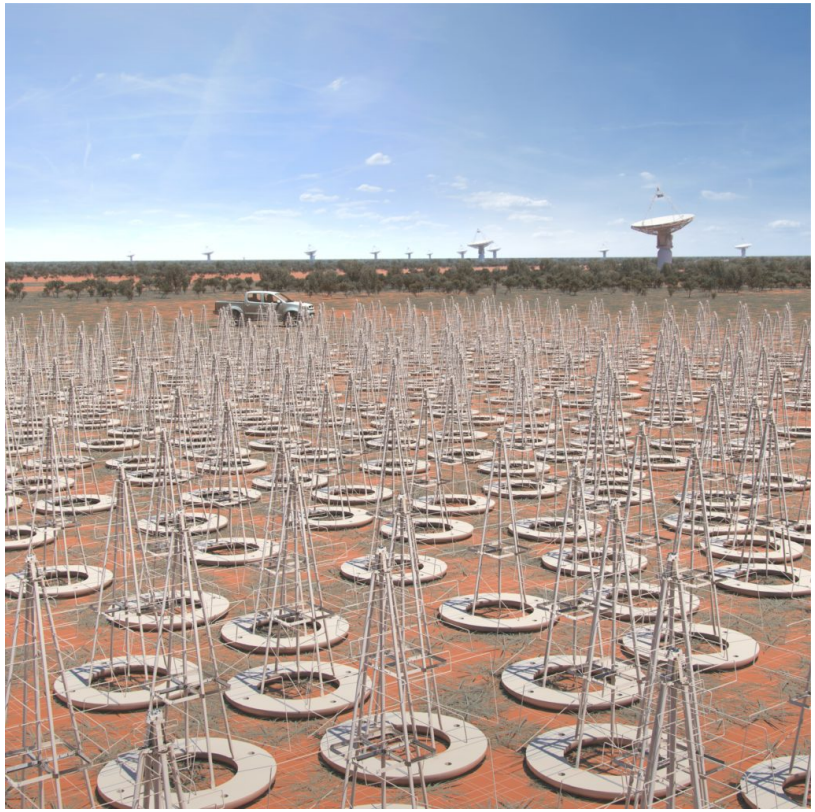

Hundreds of thousands and eventually up to a million low-frequency antennas will be located in Western Australia

Hundreds and eventually thousands of mid to high frequency 15m dishes will be located in South Africa and Africa

Credit: https://www.skatelescope.org/the-ska-project/

Parameters for the SKA precursors and pathfinders

(according to SKA-TEL-SKO-DD-001Revision:1, SKA1 System Baseline Design, P. E. Dewdney et al. 2013)

	UK	Europe (Italy! Medicina)	South Africa	West Australia
	eMERLIN	LOFAR	MeerKAT	ASKAP
A_{eff}/T_{sys} (m^2/K)	60	61	321	65
FoV (deg^2)	0.25	14	0.86	30
Receptor Size (m)	25	39	13.5	12
Fiducial frequency (GHz)	1.4	0.12	1.4	1.4
Survey Speed FoM ($deg^2 m^4 K^{-2}$)	$9.00 \cdot 10^2$	$5.21 \cdot 10^4$	$8.86 \cdot 10^4$	$1.27 \cdot 10^5$
Resolution (arcsec)	$(10\text{-}150) \cdot 10^{-3}$	5	11	7
Baseline or Size (km)	217	100	4	6
Frequency Range (GHz)	1.3-1.8, 4-8, 22-24	0.03 – 0.22	0.7-2.5, 0.7-10	0.7-1.8
Bandwidth (MHz)	400	4	1000	300
Cont. Sensitivity (μJy-$hr^{-1/2}$)	27.11	266.61	3.20	28.89
Sensitivity, 100 kHz (μJy-$hr^{-1/2}$)	1714	1686	320	1582
SEFD (Jy)	46.0	45.2	8.6	42.5

Parameters for SKA

(according to SKA-TEL-SKO-DD-001Revision:1, SKA1 System Baseline Design, P. E. Dewdney et al. 2013)

	SKA1-SUR	SKA1-LOW	SKA-MID
A_{eff}/T_{sys} (m^2/K)	391	1000	1630
FoV (deg^2)	18	27	0.49
Receptor Size (m)	15	35	15
Fiducial frequency (GHz)	1.67	0.11	1.67
Survey Speed FoM ($deg^2 m^4 K^{-2}$)	$2.75 \cdot 10^6$	$2.70 \cdot 10^7$	$1.30 \cdot 10^6$
Resolution (arcsec)	0.9	11	0.22
Baseline or Size (km)	50	50	200
Frequency Range (GHz)	0.65 – 1.67	0.050 – 0.350	0.35 – 14
Bandwidth (MHz)	500	250	770
Cont. Sensitivity (μJy-$hr^{-1/2}$)	3.72	2.06	0.72
Sensitivity, 100 kHz (μJy-$hr^{-1/2}$)	263	103	63
SEFD (Jy)	7.1	2.8	1.7

Table 1: Outline of Reference Surveys

#	Science Drivers	ν_{obs} (GHz)	Tier	rms (μJy/b)	Area (deg^2)	θ (")	Increment over pre-SKA
1	SFHU AGN/gal co-evolution	$\sim 1^a$	Ultra Deep	0.05	1	0.5[b]	40× deeper than VLASS-3; 10× smaller area; similar resolution
			Wide	1	1-5 10^3	0.5	Same sensitivity as MIGHTEE-2 survey; 30 – 100× larger area; 8× higher resolution
			Deep	0.2	10-30	0.5	10× deeper than VLASS-3; same area; similar resolution
2	SFHU AGN/gal co-evolution	~ 10	Ultra Deep	0.03	0.008	0.1	20× deeper than JVLA 8 GHz GOODS-N field; similar area; 2× better resolution
			Deep	0.3	0.5	0.05	2× deeper than 5 GHz tier of eMERGE legacy survey; 20× larger area; same resolution
3	Non-thermal emission in Clusters and Filaments	0.12	All-sky	$\sim 20^c$	31 10^3	10	3× better surface brightness sensitivity than LOFAR all sky surveys, corresponding to the detection of 10× fainter radio halos/relics
4	Strong Gravitational Lensing	1.4	All-sky	3	31 10^3	≤ 0.5	~ 100× more radio-loud strong GL than currently known; ~ 10× more lens systems than the total current sample at all wavelengths
	Legacy/Rare Serendipity			2		~ 2	5× deeper sensitivity than ASKAP all sky survey (EMU); 5× better angular resolution

[a] Reference value. The observing frequency can be fine-tuned within Band 1 and/or 2
[b] Reference value at 1 GHz. < 1 arcsec required to avoid confusion (see text)
[c] may be confusion limited (see Appendix)

From I. Prandoni & N. Seymour 2014

Ultra-deep source number counts (useful also for intermediate/ small scale foregrounds vs 21cm & FF & E/B modes)

All-sky surveys (useful also for Galactic foregrounds for all above topics)

Redshifted 21-cm line

21-cm line: spin-flip transition in the ground state of neutral hydrogen

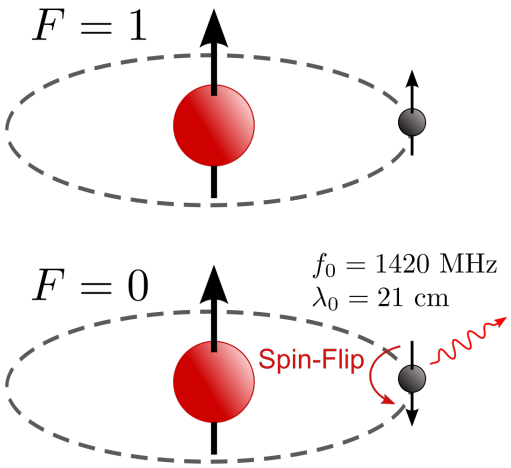

Assuming CMB assumed as a backlight

- if $T_S < T_{CMB}$ the gas is seen in absorption
- if $T_S > T_{CMB}$ the gas is seen in emission

Note: in principle T_{CMB} can be replaced by any possible background radiation

$$\delta T_b(\nu) = \frac{T_S - T_{\rm CMB}}{1+z}\left(1 - e^{-\tau_{\nu_0}}\right)$$

$$\simeq 27 x_{HI}\left(1 - \frac{T_{\rm CMB}}{T_S}\right)(1+\delta_{nl})\left(\frac{H(z)}{d\nu_r/dr + H(z)}\right)\sqrt{\frac{1+z}{10}\frac{0.15}{\Omega_M h^2}}\left(\frac{\Omega_b h^2}{0.023}\right)\ \text{mK}$$

$\delta_{nl}(\vec{x}, z) \equiv \rho/\bar{\rho} - 1$ evolved (Eulerian) density contrast

$d\nu_r/dr$ comoving gradient of the line of sight component of the comoving velocity

Furlanetto et al. 2006, Phys. Rep.

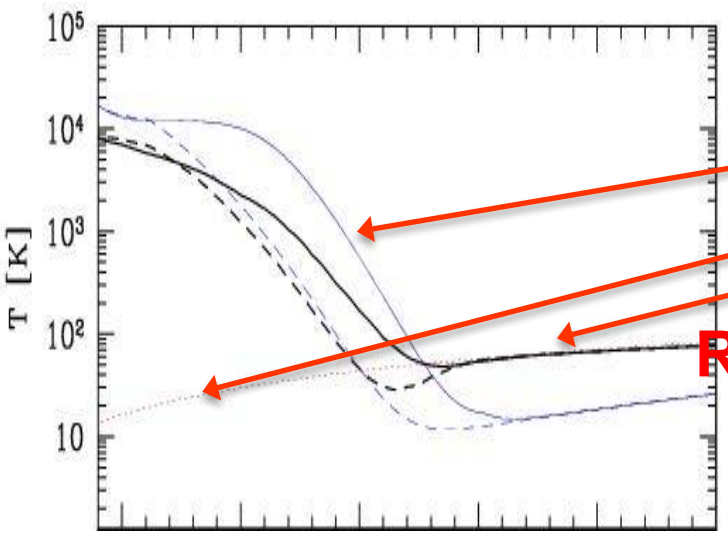

Temperatures:[kinetic, CMB, spin (21 cm)]

Reionization: synergy CMB-21cm

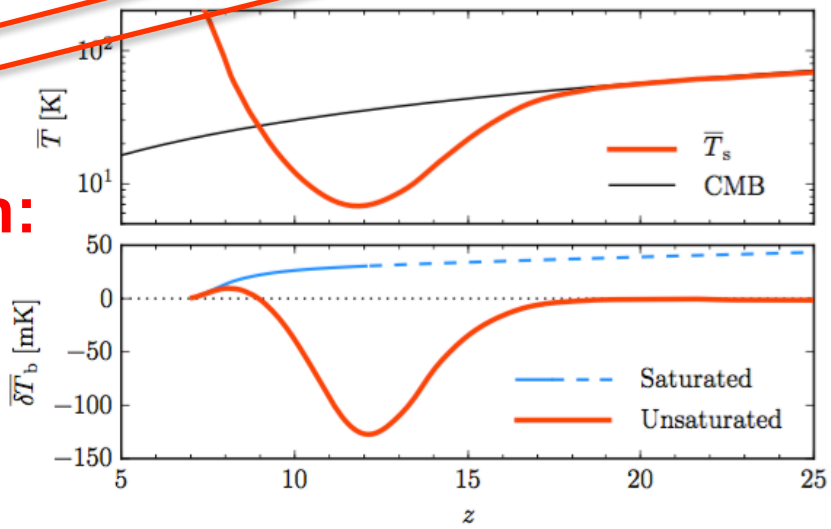

From Schneider et al. 2008, MNRAS, 384, 1525

From Geil et al et al. 2017 (Mesinger et al 2016)

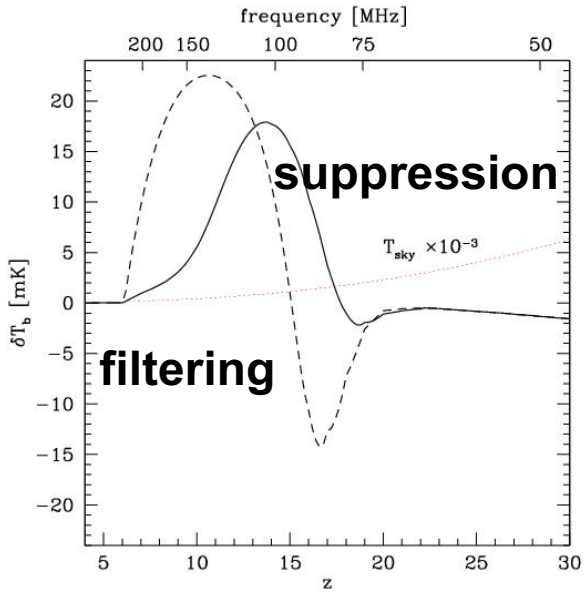

Possible predictions for 21-cm global signal according to T_S evolution

21cm require removal of foreground at a few x 10^{-3} level

21cm signal: detectability filtering - suppression

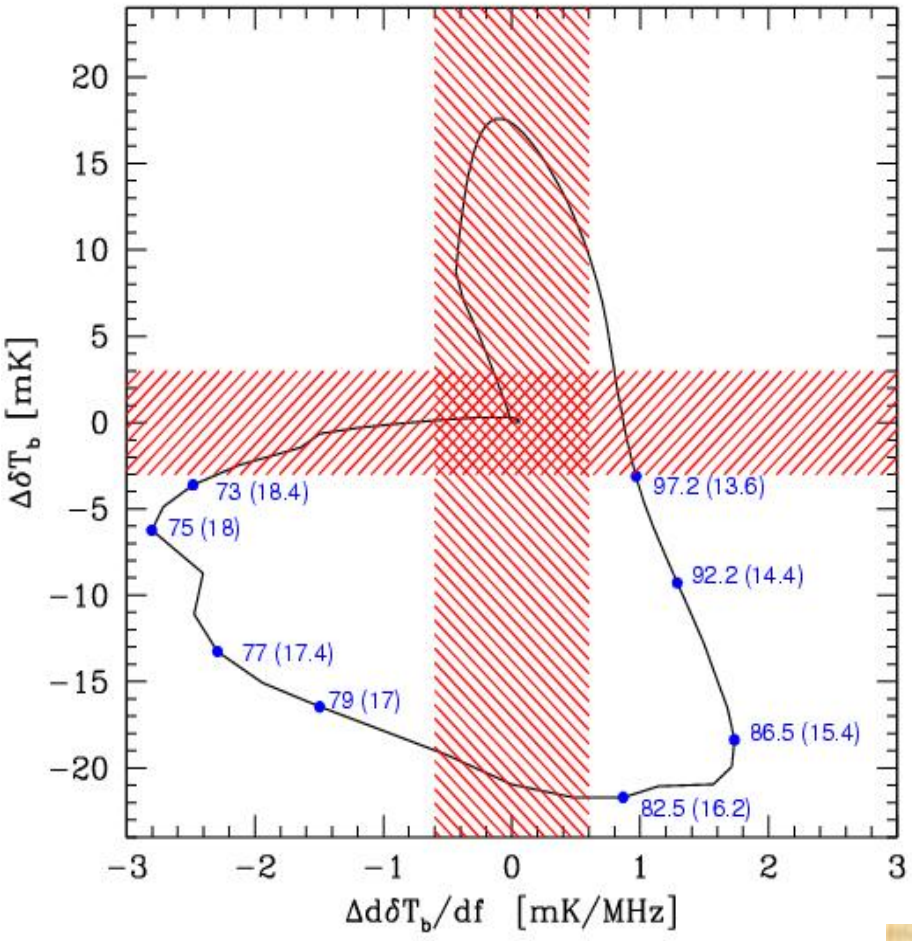

A successful detection requires:

$\Delta\delta T_b > 3$ mK

$\Delta(d\ \delta T_b/df) > 0.6$ mK MHz^{-1}

Single-dish, all sky 21cm observations can discriminate between the two model in the frequency ranges

ν_{obs} = 73-79 MHz (z=17-18.4)

ν_{obs} = 82.5-97.2 MHz (z=13.6-16.2)

From Schneider et al. 2008, MNRAS, 384, 1525

Category	Cooling Channel	f_*	f_X	SED	τ
Standard Case (1 model)	Atomic cooling	0.05	1	Hard SED	0.066
Small Variations (32 models)	Molecular cooling Massive cooling	$0.05 \times \sqrt{10}$ $0.05/\sqrt{10}$	$\sqrt{10}$ $1/\sqrt{10}$	Hard SED & Mini-quasars Soft SED & Mini-quasars	0.066 0.082
Large Variations (20 models)	Metal cooling Super-massive cooling	0.5 0.005	0.1 10	Soft SED Mini-quasars	0.066 0.098
Space filler (106 models)	Molecular cooling Atomic cooling Massive cooling	0.005 0.05 0.5	0.1 1 8	Soft SED Hard SED	0.066 0.082
Fialkov et al. (2016) (22 models)	Atomic cooling Massive cooling	0.05	lower limit 1 upper limit	Soft SED Hard SED Mini-quasars	0.06 – 0.11

Table 1. Summary of the considered models. The name of the category of models appears in the first column, for reference. We vary the cooling channel (column 2), star formation efficiency (f_*, column 3), X-ray efficiency of X-ray sources (f_X, column 4), spectral energy distribution of X-ray sources (SED, column 5), and the total CMB optical depth (τ, column 6), taking various combinations of the various parameters within each category. For each cooling channel, we use all the possible combinations of the parameters f_*, f_X, SED and τ that are listed in the same category. Note that some of the parameter combinations are ruled out by PAPER measurements and/or they produce only very large $\tau > 0.098$ and thus fail our normalization criterion. These models are included here but are excluded from our results. Also, in the Fialkov et al. (2016) category, each case has a different lower and upper limit on f_X (see Section 3.2). A complete listing of the details of all the included models is given in Appendix A.

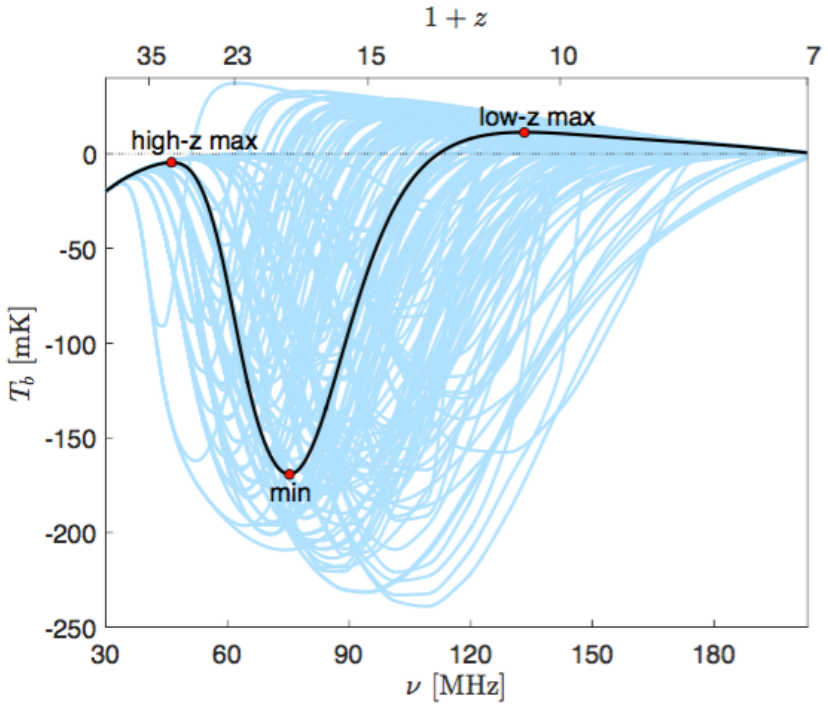

Cohen et al. 2016

Wide range of possibilities!

Wide envelope of possible predictions

- ✓ negative signals up to ~ −250mK
- ✓ positive signals up to ~ 50mK

peaking at frequencies located in a wide range between ~ 50 and 150 MHz corresponding to z ~ 30 to 10

21-cm fluctuations

- ✓ **Extensive simulation work on the evolution of the 21-cm structure during cosmic dawn age and EoR using the code 21CMFAST12 (Mesinger et al., 2011)**
  (21cm flucts recently implemented also in CAMB)
- ✓ ***Planck* 2015 measurement of τ**
- ✓ **Calibrated, sub-grid prescriptions for inhomogeneous recombinations and photo-heating suppression of star formation in small mass galaxies, with the efficiency of SNe feedback set as a free parameter to produce sets of simulations accounting for a suitable range of faint unseen galaxies**

- ✓ **The duration of reionization is predicted to be in the range $2.7 < \Delta z_{re} < 5.7$**

- ✓ **The large-scale 21-cm power during the advanced EoR stages can be different by up to an order of magnitude, according to the model**
- ✓ **The main difference due to the typical bias of sources and the more efficient negative feedback in models with an extended EoR driven by faint galaxies**

- ✓ **The Faint Galaxies model simulation corresponds to the limit of inefficient or halo-mass independent SNe feedback, with star forming galaxies hosted mainly by fairly small halos close to the atomic cooling threshold of virial temperature $T_{vir} \sim 10^4$ K, implying that the dominant galaxies are relatively abundant, with a small bias, an early formation and a slow evolution**

21-cm fluctuations

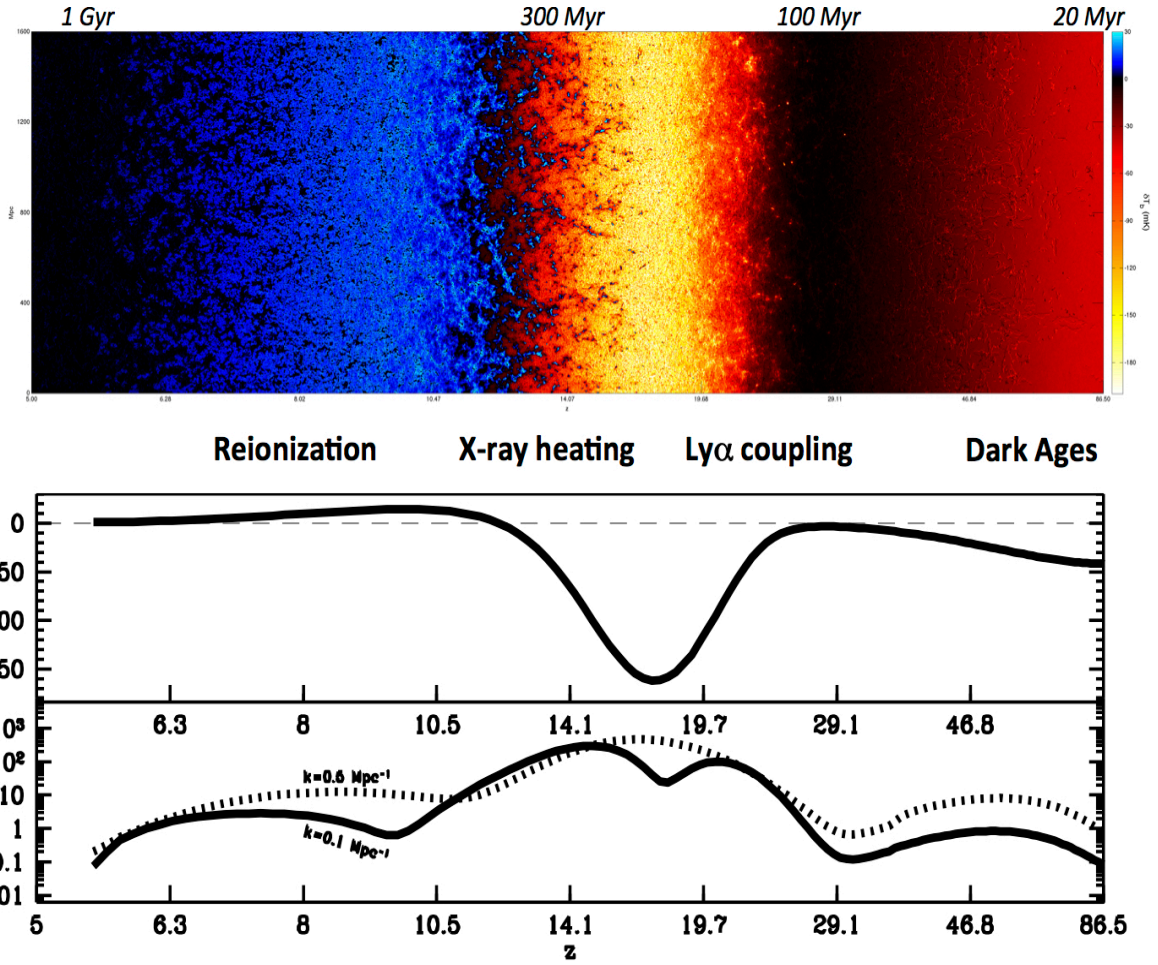

Mesinger et al. 2016, MNRAS

Evolution of the 21-cm *power spectrum* reflects the midpoints of the sequence of the three main astrophysical epochs corresponding to

- ✓ Lyman-α pumping
- ✓ X-ray heating
- ✓ EoR

The throughs in the large-scale power evolution roughly correspond to the boundaries between three main phases following Dark Ages

The EoR peak occurs somewhat after the midpoint, due to the overlap between X-ray heating and EoR

Constraints on parameters ("astrophysical sector" forecasts for a 5 parameter space)

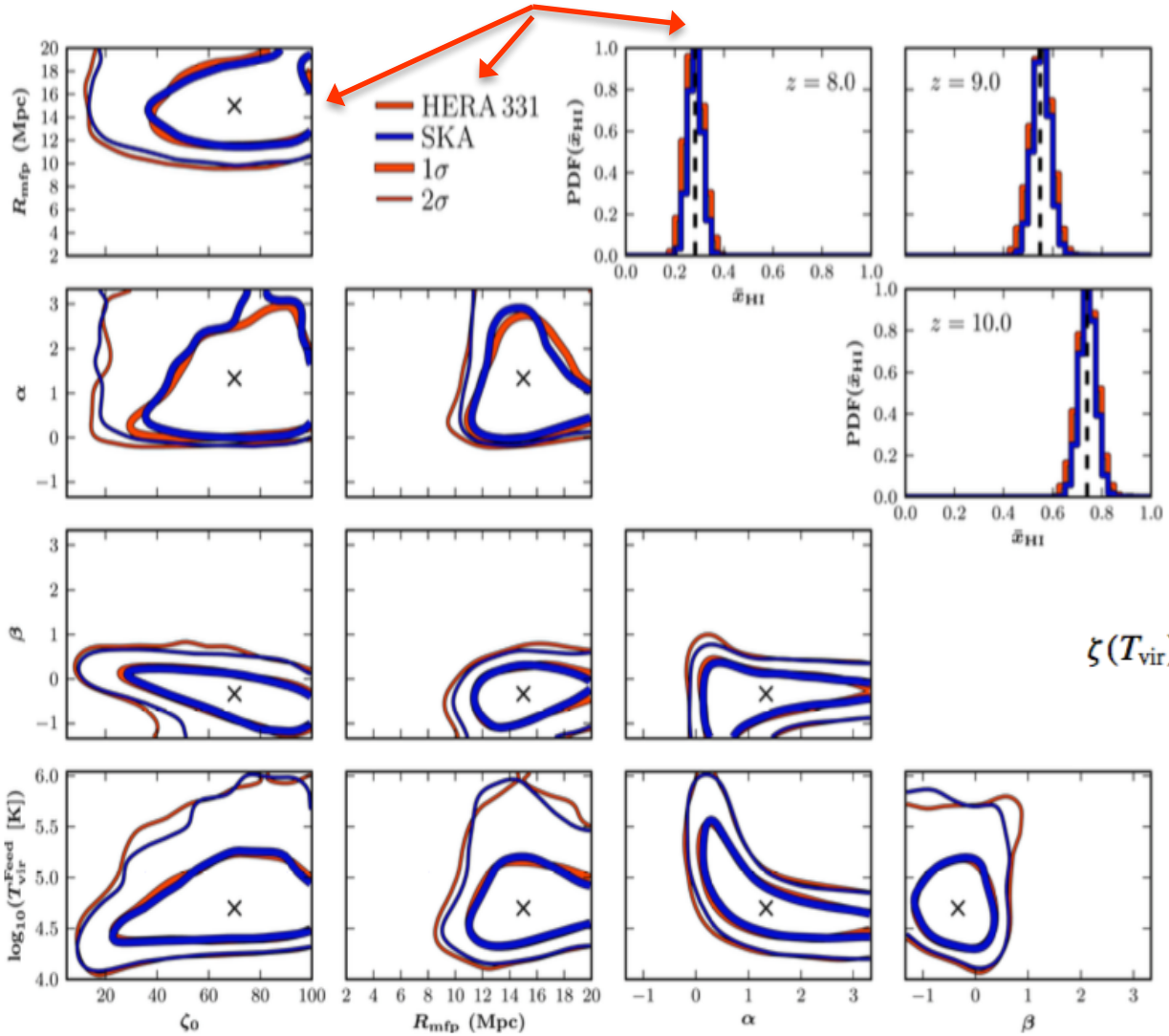

R_{mfp} = mean free path of ionizing photons within ionized regions

T^{Feed}_{vir} = minimum virial temperature of star-forming haloes

ζ = *Ionizing efficiency*

$$\zeta(T_{\rm vir}) = \zeta_0 \begin{cases} \left(\frac{T_{\rm vir}}{T_{\rm vir}^{\rm Feed}}\right)^{\beta} & T_{\rm vir} \geq T_{\rm vir}^{\rm Feed} \\ \left(\frac{T_{\rm vir}}{T_{\rm vir}^{\rm Feed}}\right)^{\alpha} & 10^4\,{\rm K} \leq T_{\rm vir} < T_{\rm vir}^{\rm Feed} \\ 0 & T_{\rm vir} < 10^4\,{\rm K}. \end{cases}$$

+ a certain role in the estimation (with CMB and other probes) of σ_8 or equivalent parameter

Greig & Mesinger 2015, MNRAS

But … two surprises: 1. Arcade 2

"We conclude that the residual signature is due either to a diffuse extragalactic background of emission from discrete radio sources with properties somewhat different than the faint end of the distribution of known sources or to unmodeled residual emission from our own Galaxy. Although we believe the former to be more likely, we cannot exclude the latter explanation. Further observations with sufficient sensitivity to distinguish between these on the basis of spectral index may clarify which explanation is correct."
(Seiffert et al. 2011)

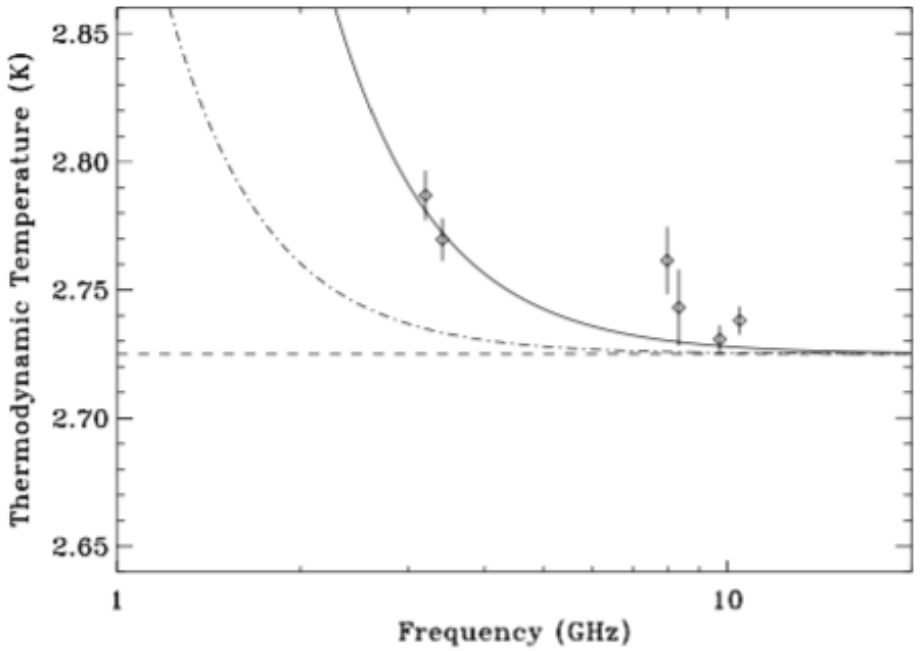

Figure 1. Detection of radio emission by ARCADE 2 beyond the contribution of discrete radio sources, modeled galactic foregrounds, and the expectation of 2.725 K blackbody radiation. Data points are the ARCADE 2 results from Fixsen et al. (2011) and have been corrected for Milky Way Galactic emission described by Kogut et al. (2011). The dashed curve is a constant 2.725 K blackbody, consistent with FIRAS measurements of the CMB. The dot-dashed curve is an estimate of the discrete radio source contribution from Gervasi et al. (2008a) model "Fit1" added to the 2.725 blackbody. The data points lie significantly above this dot-dashed curve, indicating our detection of excess emission. The solid curve is the best fit of the combined data of Table 1 and FIRAS to a power law plus a constant CMB temperature.

But … two surprises: 2. EDGES

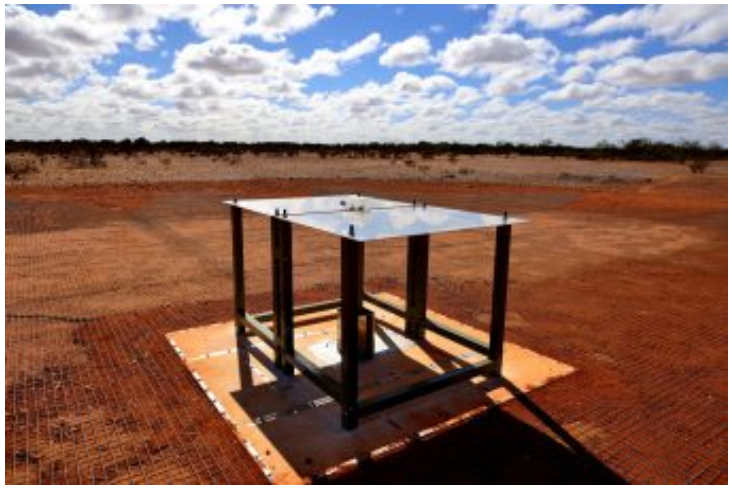

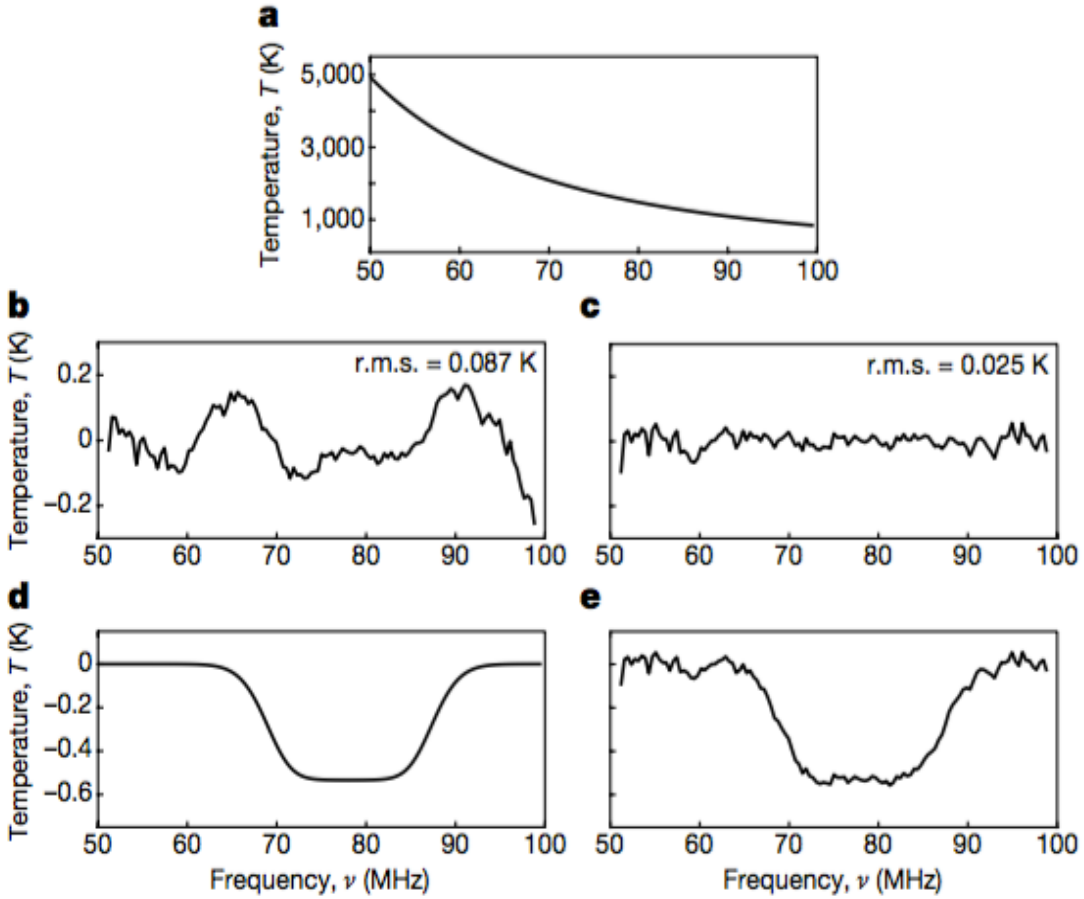

Figure 1 | Summary of detection. a, Measured spectrum for the reference dataset after filtering for data quality and radio-frequency interference. The spectrum is dominated by Galactic synchrotron emission. **b**, **c**, Residuals after fitting and removing only the foreground model (**b**) or the foreground and 21-cm models (**c**). **d**, Recovered model profile of the 21-cm absorption, with a signal-to-noise ratio of 37, amplitude of 0.53 K, centre frequency of 78.1 MHz and width of 18.7 MHz. **e**, Sum of the 21-cm model (**d**) and its residuals (**c**).

Bowman et al. 2018, Nature

EDGES 21-cm monopole

- ✓ Set of observational campaigns, started in August 2015, carried out with low-band instruments of the Experiment to Detect the Global Epoch of Reionization Signature (EDGES)
- ✓ Surprisingly, a pronounced absorption profile, with an almost symmetric U-shape, centred at 78±1 MHz (Bowman et al. 2018)
- ✓ Amplitude of the absorption feature of 0.5K (+0.5K,−0.2K) more than a **factor of two greater** than those predicted by the most extreme astrophysical models
- ✓ The spread of the profile has a FWHM of 19+4 MHz, the low-frequency edge supporting the existence of a ionizing background by 180 million years after the Big Bang
- ✓ The high-frequency edge indicating that the gas was heated to above the radiation temperature less than 100 million years later

Consistent with limits by Large aperture Experiment to detect the Dark Ages (LEDA)

signal amplitude between −890 and 0 mK at 95% C.I. in the frequency range $100 > \nu > 50$ MHz corresponding to a range $13.2 < z < 27.4$ (with a width > 6.5 MHz corresponding to a spread in $z > 1.9$ at $z \sim 20$)

Bernardi et al. 2016

Possible explanations - I

Explanations of the profile amplitude are very intriguing

➢ **The primordial gas was much colder than expected**

e.g. gas cooling model caused by interactions between DM and baryons (Barkana, 2018; Munoz and Loeb, 2018)

Barkana, 2018: combination of radiation from the first stars and excess cooling of the cosmic gas induced by its interaction with dark matter

Original example: cross-section for baryon–DM collisions expressed with respect to a relative velocity normalized, with dependence as in Rutherford (or Coulomb) scattering

$$\sigma(v) = \sigma_c \left(\frac{v}{c}\right)^{-4} = \sigma_1 \left(\frac{v}{1\,\mathrm{km\,s^{-1}}}\right)^{-4}$$

- **Non-standard Coulomb-like interaction between DM particles and baryons**: does not depend on whether the baryons are free or bound within atoms.
- Thermal evolution of baryons and DM by following the exchange of energy and momentum between them, in which their relative velocity after cosmic recombination has an important role.
- Velocity remnant arises from the fact that
  - ✓ motion of DM is determined by gravity, whereas
  - ✓ baryons scatter rapidly off the CMB photons and move along with them in their acoustic oscillations prior to cosmic recombination

- By combining baryon–DM scattering with radiation emitted from the first stars during cosmic dawn, Barkana found strong 21-cm absorption that can explain the feature measured by EDGES

Barkana 2018, Nature

- This absorption dip can be attributed to early astrophysically generated Lyman-α and X-ray radiation backgrounds, consistently with observations (no detection of strong absorption signal at higher frequencies)

- The unexpectedly large depth of the 21-cm absorption indicates cosmic gas that has been cooled substantially by baryon–DM scattering

→ only a combination of the two ideas can account for the EDGES data

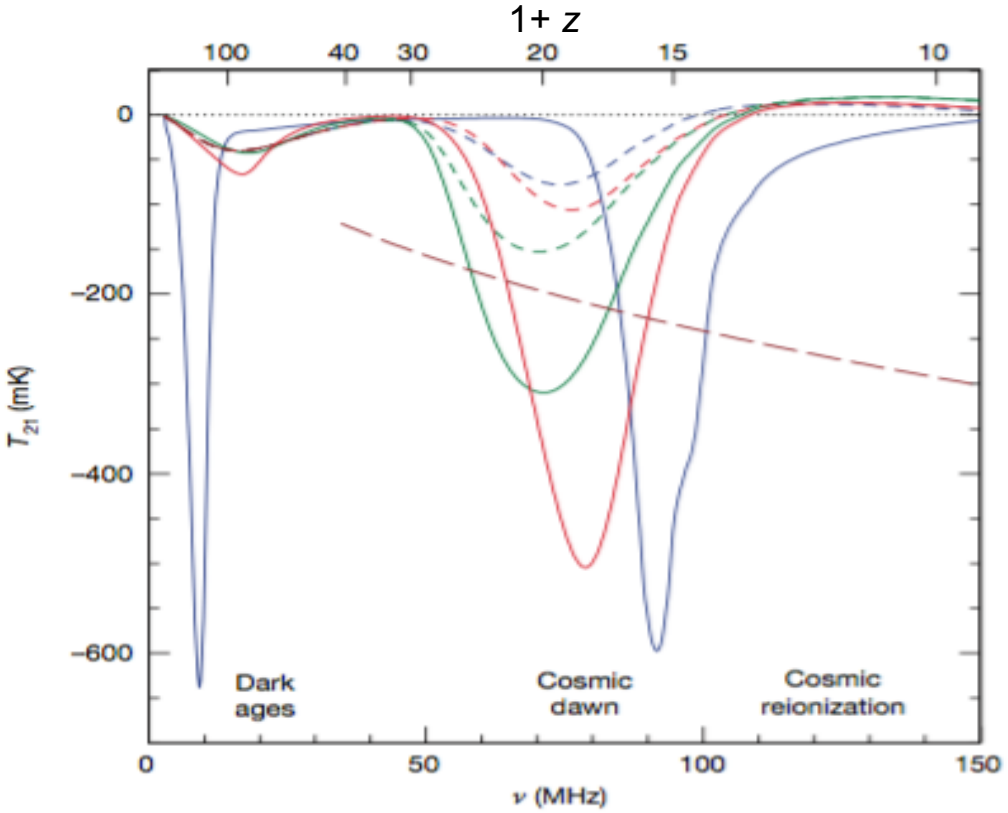

Figure 2 | Global 21-cm signal in models with baryon–dark matter scattering. The globally averaged 21-cm brightness temperature T_{21} (in millikelvin) is shown at an observed frequency ν (in megahertz), with the corresponding value of $1+z$ displayed at the top. We chart some of the space of possible 21-cm signals (see Methods for a discussion on their shapes) using three models (solid curves), with: $\sigma_1 = 8 \times 10^{-20}$ cm^2 and $m_\chi = 0.3$ GeV (red; roughly matching the most likely observed value[5] of the peak absorption); $\sigma_1 = 3 \times 10^{-19}$ cm^2 and $m_\chi = 2$ GeV (green); and $\sigma_1 = 1 \times 10^{-18}$ cm^2 and $m_\chi = 0.01$ GeV (blue). The astrophysical parameters assumed by these models are given in Methods. The corresponding 21-cm signals in the absence of baryon–dark matter scattering are shown as short-dashed curves. Also shown for comparison (brown long-dashed line) is the standard prediction for future dark ages measurements assuming no baryon–dark matter scattering for $\nu < 33$ MHz (matches all the short-dashed curves in this range) and the lowest global 21-cm signal at each redshift that is possible with no baryon–dark matter scattering, regardless of the astrophysical parameters used (for $\nu > 33$ MHz).

Possible explanations - II

Explanations of the profile amplitude are very intriguing

- **The background radiation temperature was hotter than expected**

owing to a substantial contribution by a high-z, faint population of radio sources as proposed by Feng and Holder (2018) in line with the interpretation of the signal excess found by ARCADE 2 (Seiffert et al., 2011)

or in the model by Ewall-Wice et al. (2018), involving a radio background, overwhelming that of the CMB, generated by black hole remnants of Pop-III stars at z ≈ 17 from black holes formed at higher z,
and heavily obscured or with a radio loud fraction larger than that in the local Universe in order to avoid high τ values ruled out by *Planck*, with strong emission and growth declining at z < 16

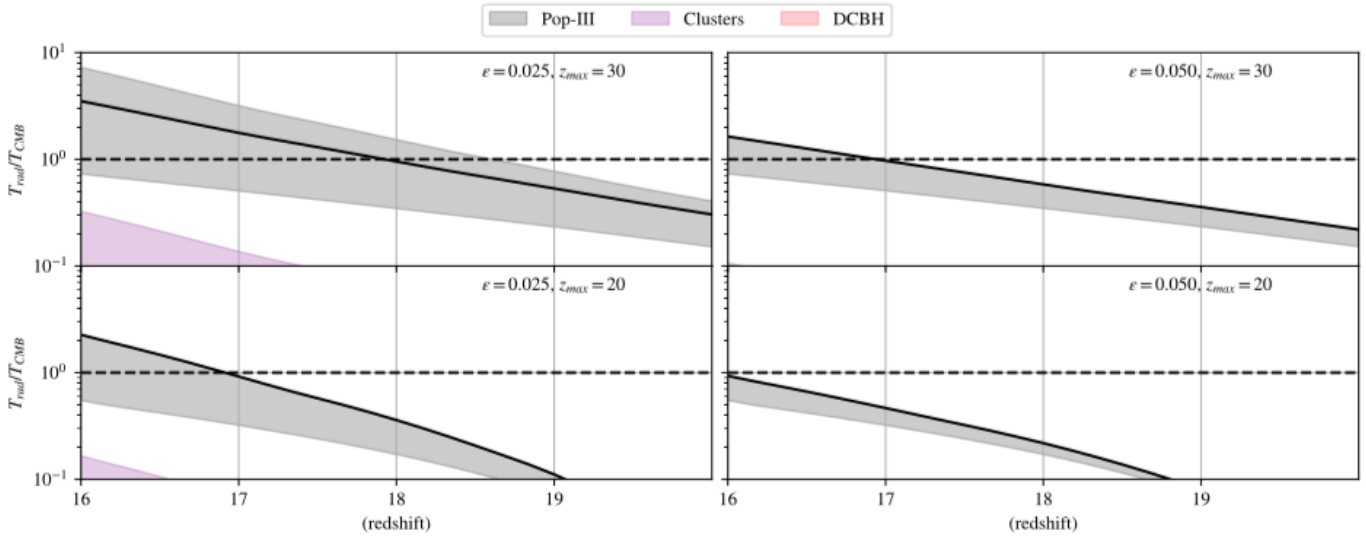

FIG. 1.— The ratio between $T_{\rm rad}$ and $T_{\rm CMB}$, as a function of redshift for various values of z_{max} and ϵ. The filled shaded regions denote the range of temperatures predicted between $f_{\rm edd} = 10^{-2}$ and 1 for our DCBH (red), Cluster collapse (purple), and Pop-III (black) scenarios (see table 1). For fixed $z_{\rm max}, \epsilon$, we also plot the maximum $f_{\rm edd}$ curve allowed by the CXB (Fig. 3) as a solid line. In the absence of heating effects, models that pass above the horizontal dashed line at $z \lesssim 17$ are producing a sufficient radio background to account for the absorption feature detected by the EDGES experiment.

(DCBH= Direct Collape Black Holes)

High ratio between "source background" and CMB background

Ewall-Wice et al. 2018

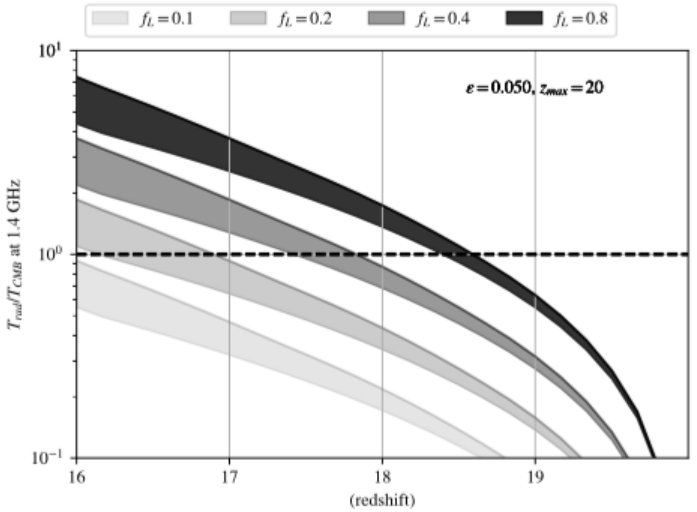

FIG. 7.— The same as Fig. 1 but now only considering Pop-III black holes, and fixing $\epsilon = 0.05$ $z_{\rm max} = 20$ to meet Planck Collaboration et al. (2016) optical depth requirements for large escape fractions (Fig. 6). Doubling the radio-loud fraction from what is observed at the present day gives us enough emission to produce the EDGES absorption feature.

Experiments to improve global (monopole) signal by the cosmic dawn and the EoR:

- ✓ LEDA
- ✓ EDGES
- ✓ Sonda Cosmologica de las Islas para la Deteccion de Hidrogeno Neutro (SCI-HI) (Voytek et al., 2014)
- ✓ Probing Radio Intensity at high z from Marion (PRIZM)
- ✓ Shaped Antenna measurement of the background Radio Spectrum 2 (SARAS 2) (Singh et al., 2017)

Interferometric facilities promise a next identification of redshifted 21-cm fluctuations:

- ✓ LOFAR, 21
- ✓ CentiMeter Array (21CMA) (Huang et al., 2016)
- ✓ Murchison Widefield Array (MWA) (Jacobs et al., 2016; Beardsley et al., 2016)
- ✓ Hydrogen Epoch of Reionization Array (HERA) (DeBoer et al., 2017)
- ✓ Donald C. Backer Precision Array for Probing the Epoch of Reionization (PAPER) (Cheng et al., 2016)
- ✓ Expansion of existing Long Wavelength Array station (Dowell et al., 2017)
- ✓ SKA: with a frequency coverage of ~70–200 MHz, SKA-LOW would be able to cover the entire EoR, but, likely, also the epoch of IGM heating

Sky complexity

rms fluctuations in T & P: CMB vs foregrounds

Change of paradigm from *Planck* maps

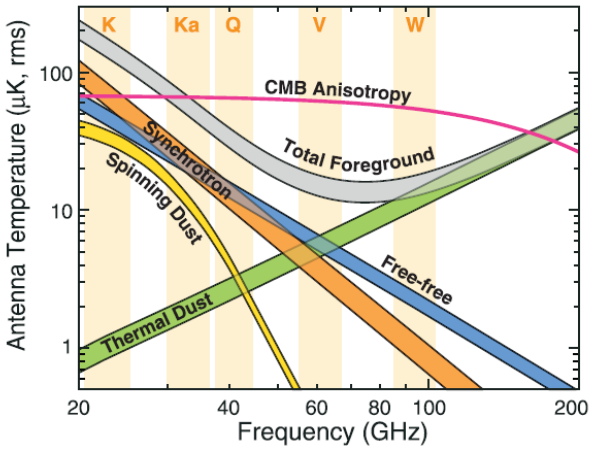

WMAP 9

75-85% sky coverage

***Planck* in T:** 81-93% sky coverage - 1° FWHM

c.f. common mask 78%

Microwave sky complexity: more relevant components!

Many parameters!

Synch: 2 +
Dust: 3 (* 2 ?)
FF: 2 (EM,T_e)
Spinning dust: 3loc+1glob

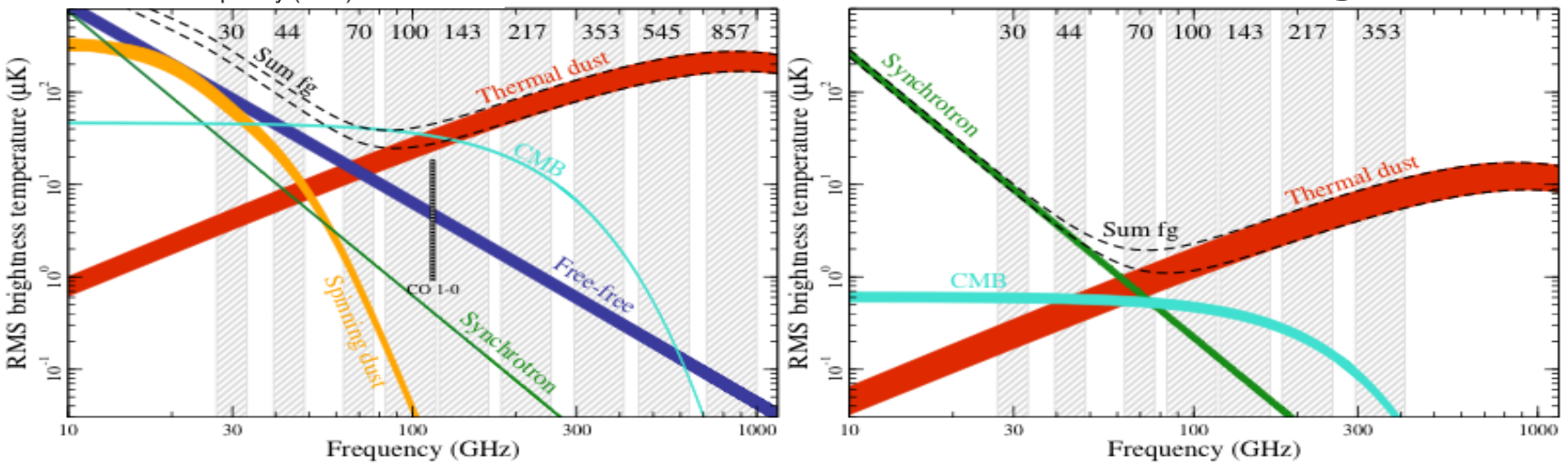

Fig. 16. Brightness temperature rms as a function of frequency and astrophysical component for temperature (*left*) and polarization (*right*). For temperature, each component is smoothed to an angular resolution of 1° FWHM, and the lower and upper edges of each line are defined by masks covering 81 and 93 % of the sky, respectively. For polarization, the corresponding smoothing scale is 40′, and the sky fractions are 73 and 93 %.

Low frequency Galactic foregrounds

The accurate study of Galactic emissions is crucial for any cosmological exploitation of radio to infrared sky.

As first probed by DASI, interferometers can be fruitfully used to map the diffuse sky signal on relatively wide areas in both total intensity and polarization, Fourier transforming data from the U-V space to the real 2D space

- The possibility of extending this opportunity to intermediate and large scales (low and intermediate multipoles) largely relies on the capability of available mosaic techniques to assemble different FoVs into maps with appropriate large scale calibration and matching

- This is of increasing complexity at SKA increasing frequency, since the smaller FoV sizes of higher frequencies

- **Also, recalibration of SKA FoVs with precursors (ASKAP-PAF, Meerkat) maps could be in principle exploited**

- On the other hand, the high Galactic radio signal does not require the extreme accuracy demanded, for instance, by CMB fluctuation mapping at the SKA highest frequencies

- **If mosaic techniques will work successfully, a view of a very wide sky fraction will allow to map Galactic foregrounds at intermediate and large scales. This will have a tremendous impact for 3D physical models of the Galaxy and for the study of the large scale, almost regular component of the Galactic magnetic field**

- **Turbulence phenomena predict a typical power law dependence of the power spectrum of diffuse emission with properties related to the physical conditions of the ISM in the considered area**

- **Almost independently of the accuracy of mosaic techniques, SKA maps on many patches of sky of limited area will allow to reconstruct with unprecedented accuracy the correlation properties of the radio sky diffuse emission, thus providing crucial information for the comparison with theoretical models and and their implementation through numerical codes**

Multifrequency, high sensitivity radio observations with the SKA will certainly put a firm light on this problem, allowing to disentangle between the various depolarization effects:

- **Faraday depolarization associated to Galactic magnetic fields**
- **geometrical depolarization coming from the averaging in the observed signal of contributions from cells with different polarization angles:**

  - ✓**along the line of sight**
  - ✓**within the angular directions of the observational effective beam**

Two other topics crucial for both Galactic science and foreground treatment for cosmology are the understanding of:

- ✓**anomalous microwave emission**
- ✓**haze component**

SKA will map the low frequency tail of these emissions

The relevance of extragalactic foregrounds

- Emerged clearly in ARCADE 2 … and EDGES
- Although these signals and their interpretations are controversial, they underline how crucial is the precise estimation of very faint source counts

- The SKA sensitivity at 20 GHz will allow the detection (to 5σ) of sources down to a flux level of ≃ 200 nJy (≃ 60,20,6 nJy) in 1 (10, 10^2, 10^3) hour(s) of integration over the ≃ 1 mas (FWHM) resolution element; similar numbers (from ≃ 250 to 8 nJy in an integration time from 1 to 10^3 hours, respectively) but on a resolution element about 10 times larger will be reached at ≈ GHz frequencies by using a frequency bandwidth of about 25%

- Therefore, the SKA accurate determination of source number counts down to very faint fluxes will be crucial for cosmology

Impact of residuals & subdominant components / features complexity in dominant components

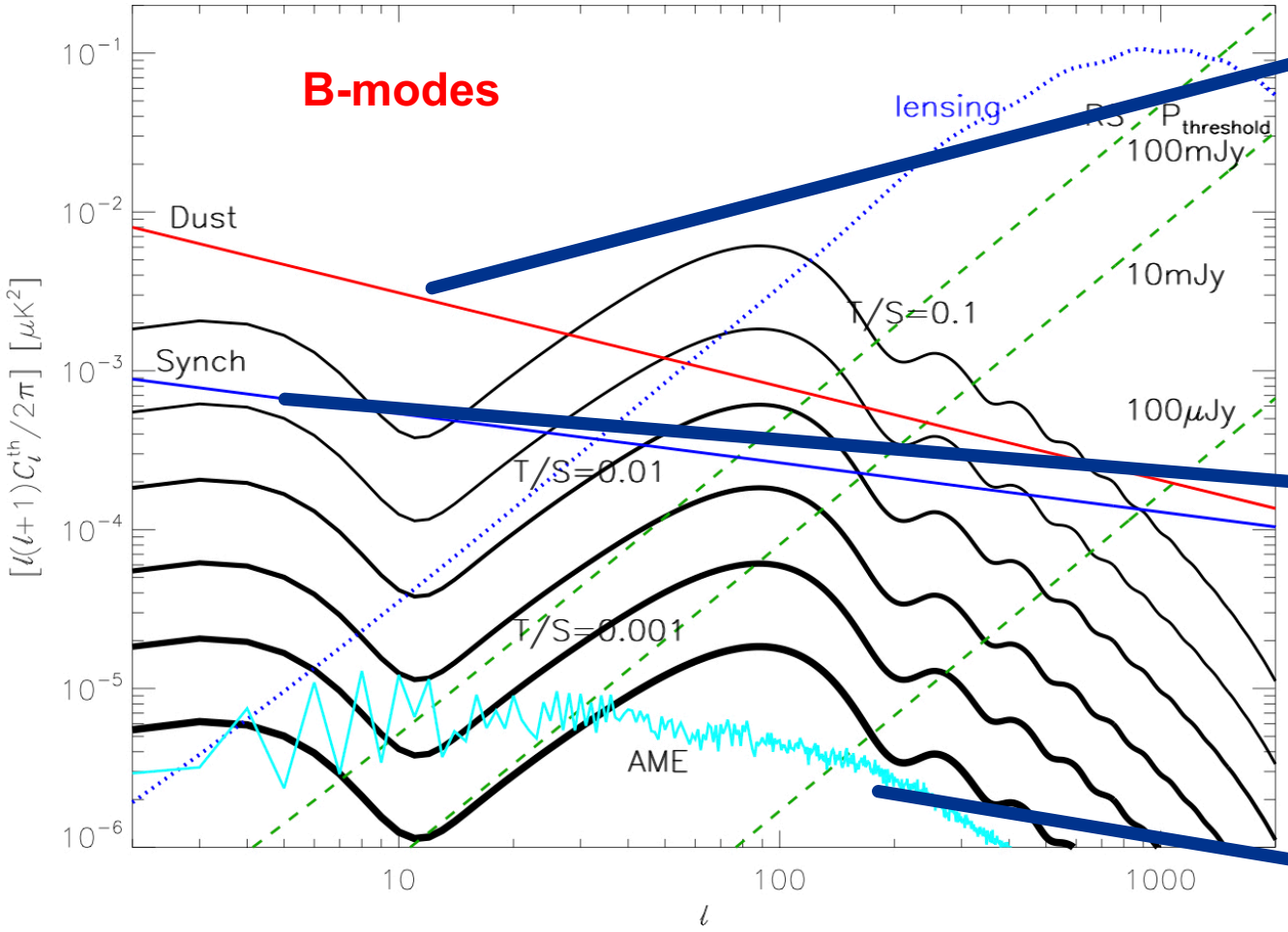

Residual from dust starting from 353 GHz for an error in beta_dust of 0.01

Residual from synch starting from 30 GHz for an error in slope of 0.02

Estimate of AME, assuming pol. degree of 2%

Trombetti & Burigana 2018, accepted, Frontiers

Galaxy @ 70 GHz from *Planck*

Sources @ 100 GHz Polarization APS from Trombetti et al. 2017

Foregrounds residuals vs CMB E-modes from reionization

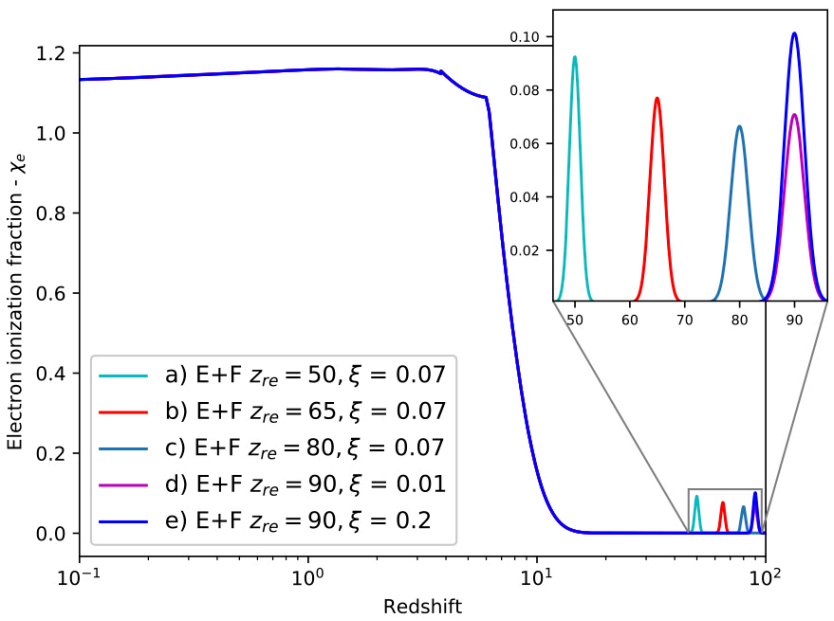

Galaxy @ 70 GHz from *Planck*

Crucial @ low/intermediate l
i.e. low redshifts

Extragal. radisources @ 100 GHz
Polarization APS from
Trombetti et al. 2017
$\Pi \simeq 2.8\%$ - IDA techniques

Crucial @ intermediate/high l
i.e. high redshifts

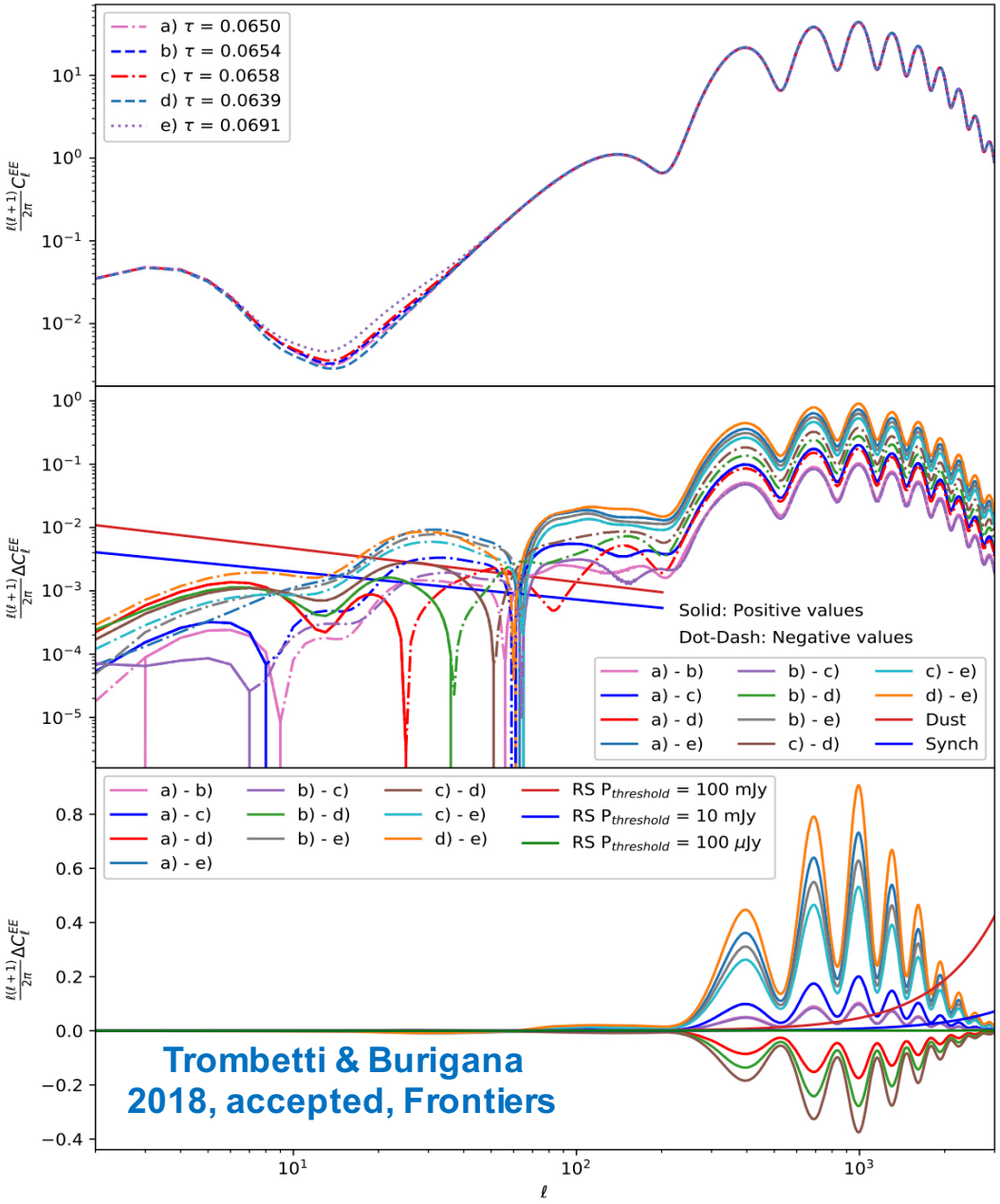

Conclusions

- **Important cosmological topics will be jointly studied with radio and microwave surveys: cosmological reionization is one of the most relevant case**

➢ **Radio: 21cm → tomography of cosmological reionization**

- **Space and ground will be more and more complementary**
- **Optimizing surveys for scientific aims is critical**
- **Reducing foreground signals and systematics is a critical and fundamental issue in practically all contexts**

Thanks to: the many colleagues of the *Planck*, CORE and SKA Collaborations; the ESA *Planck* Legacy Archive (PLA); the Legacy Archive for Microwave Background Data Analysis (LAMBDA, supported by the NASA Office of Space Science); HEALPix, CAMB authors; INAF PRIN SKA/CTA project FORmation and Evolution of Cosmic STructures (FORECaST) with Future Radio Surveys, ASI/INAF agreement n. 2014-024-R.1 for the *Planck* LFI Activity of Phase E2; ASI/Physics Department of the university of Roma–Tor Vergata agreement n. 2016-24-H.0 for study activities of the Italian cosmology community.